Z. Phys. A – Atomic Nuclei 334, 277–283 (1989)

Zeitschrift für Physik A
Atomic Nuclei

Search for Proton Radioactivity in ^{65}As, ^{69}Br and ^{77}Y

E. Hourani[1], F. Azaiez[3], Ph. Dessagne[2], A. Elayi[1], S. Fortier[1], S. Gales[1], J.M. Maison[1], P. Massolo[4], Ch. Miehe[2], and A. Richard[1]

[1] IPN, B.P. 1, Orsay, France
[2] CRN, Strasbourg, France
[3] CENBG, Le Haut Vigneau, Gradignan, France
[4] UNLP, La Plata, Argentina

Received June 19, 1989

A search for proton radioactivity in ^{65}As, ^{69}Br and ^{77}Y, produced as residues of fusion reactions, was carried out at the Orsay Tandem accelerator. The residues were collected at the image point of the spectrometer Soleno and implanted into the gaseous medium of an ionization chamber which was also used to detect the radioactivity protons. No such protons have been observed in the energy range of 250–600 keV and in the half-life interval of 10 μs–100 ms, within a production cross section sensitivity of 1 μb.

PACS: 23.90.+w; 27.50.+e; 25.70.Jj

1. Introduction

Proton radioactivity was recently discovered at Darmstadt and confirmed at Munich. Five nuclei with mass number greater than 100, i.e., ^{109}I, ^{113}Cs, ^{147}Tm and ^{150,151}Lu, have been found to be proton emitters in their ground state. Their half-lives range from a few microseconds to tenths of milliseconds and the energies of the emitted protons lie around 1 MeV. The last review on the subject is given in [1].

Because proton radioactivity is expected to be a general phenomenon for the most exotic nuclei located all along the proton rich side of the nuclear chart, we proposed to search for such a radioactivity in some nuclei in the neighbourhood of the mass number $A=70$. In particular, we selected, in a first stage, the following nuclei: ^{65}As, ^{69}Br and ^{77}Y, which are the proton richest nuclei obtainable by fusion $p2n$-evaporation reactions with $N=Z$ targets and projectiles. Indeed, experiments have been already performed for the search of proton radioactivity in ^{69}Br [2] and ^{77}Y [3] and others were announced in the case of ^{65}As and ^{69}Br [4] nuclei. Such investigations are promising since the last compilation of Wapstra et al. [5] for the atomic masses shows that most authors predict ^{65}As, ^{69}Br and ^{77}Y as the heaviest of As, Br and Y isotopes to be unstable against p radioactivity. We report in Table 1 the predicted proton separation energies which are mostly negative, reflecting thus a possible instability against p emission.

The coulomb and centrifugal barriers brought into play in proton emission by $A\approx 70$ nuclei are so low that, in case of p radioactivity, the kinetic energy of the emitted protons falls in the range of 300–500 keV corresponding to half-lives up to tenths of milliseconds. The main feature of the experiment de-

Table 1. Proton separation energies deduced from the updated list of atomic masses of Wapstra et al. [5]

Nucleus	Moller Nix	Moller et al.	Comay Kelson Zidon	Tachibana et al.	Janecke Masson	Masson Janecke	Wapstra Audi Hoekstra
^{65}As	+0.039	+0.079	−0.181	−0.011	−0.261	−0.321	−0.321
^{69}Br	−0.111	−0.131	−0.531	+0.029	−0.661	−0.631	+0.009
^{77}Y	−0.251	−0.221	−0.781	−0.171	−0.981	−0.721	–

scribed in the present paper is to be the first one in which a detection sensitivity to this energy range was reached. The fact that the previous attempts to explore the region of $A \approx 70$ were made with a high p energy threshold ($\geqq 450$ keV) strongly supports the aim of the present study.

2. Experimental Procedure

The ^{65}As, ^{69}Br and ^{77}Y nuclei were produced by fusion evaporation reactions, namely, ^{40}Ca(^{28}Si, $p2n$), ^{40}Ca(^{32}S, $p2n$) and ^{40}Ca(^{40}Ca, $p2n$). Beams of ^{28}Si, ^{32}S and ^{40}Ca were obtained at the 15 MV Orsay Tandem accelerator. A natural self-supported Ca target of 750 μg/cm^2 was used. The fusion evaporation products were collected in the focal point of the superconducting solenoidal coil Soleno [6] operating at zero degree with respect to the beam, while a good rejection for scattered projectiles of higher magnetic rigidity was obtained. The large angular acceptance of Soleno (3–10°) well adapted to the angular distribution of the fusion products allows an absolute collection efficiency of the order of 0.03–0.05 [7]. The collection time is equal to the time of flight (100–200 ns) of the ions along the distance separating the target and the detector which was placed in the image point of Soleno. The collected fusion products were implanted in the same detector destinated to detect the expected radioactivity protons, because these protons of low energy cannot escape the medium of implantation of the emitting ions.

Although the collection with Soleno of fusion evaporation products was ideal with regard to many aspects, nevertheless, there were two major difficulties left:

– at Tandem energies, the energy and charge state distributions are broad; as a consequence, the magnetic rigidity of unwanted abundant fusion products, e.g., those corresponding to $2pn$, $3p$, ... evaporation are collected in the same way than the expected proton radioactive nuclei. The ratio of non radioactive products to radioactive ones is expected to be of the order of 10^5.

– as the great part of the collected ions are β-emitters, there is a tremendous β-background at low energy, extending to around 500 keV in Si detectors, even in the thinnest ones, and to some tenths of keV in gaseous detectors; this fact made the use of Si detectors inacceptable in our experiment and lead us to construct and set up an ionization chamber whose gaseous medium served to implant heavy ions as well as to detect the emitted protons. The problem of detecting the very low amplitude signals of protons in the tail of high amplitude heavy ion signals was solved by using an especially built electronic rejection circuit placed after the preamplifier [8].

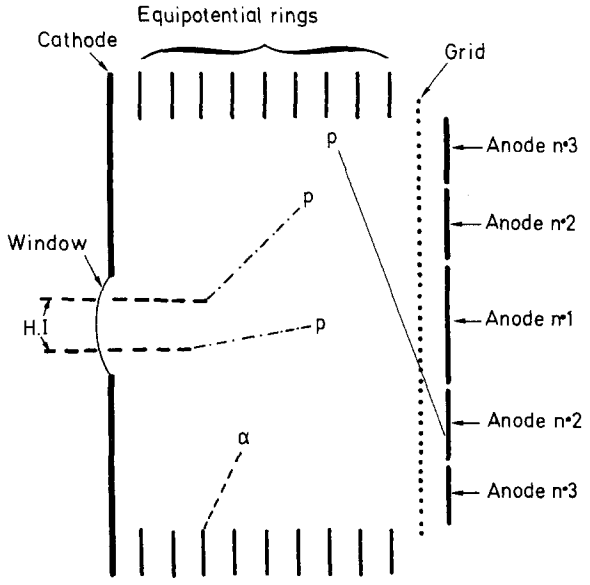

Fig. 1. Schematic drawing for the axial ionization chamber (∅ = 13 cm, h = 10 cm) used in this work. The anode is composed of three concentric compartments labelled 1, 2, and 3 of diameters 3.9, 8.8 and 13 cm respectively. Paths of heavy ions implanted in the gas are represented by thick dashed lines and those of expected radioactivity protons by dashed-dotted lines. Paths of β-delayed protons are represented by continuous thin lines and those of α-particles from natural radioactivity of materials by dashed lines

The ionization chamber was cylindrical and of axial electric field. Its anode was divided into three concentric compartments (Fig. 1). A 100 μs square-shaped pulsation of the beam was used.

Off-beam signals delivered by the ionization chamber were expected to be due to (see Fig. 1):

1) the radioactivity protons of 300–500 keV, which are searched for. The gas pressure in the chamber was chosen so that they would have ranges of 2–4 cm and hence loose their total energy in the gas, giving peaks in the energy spectrum. They should be detected either in the single energy spectrum E_1 of anode n° 1 or in the coincident energy spectrum $E_1 + E_2$ of anodes n° 1 and 2.

2) the well-known delayed protons [9–13] of energy ranging from 1 to 3 MeV originating from ^{65}Ge in case of ^{40}Ca(^{28}Si, $2pn$) reaction, from ^{69}Se in case of ^{40}Ca(^{32}S, $2pn$) and from ^{77}Sr in case of ^{40}Ca(^{40}Ca, $2pn$). These protons of relatively high energy cross the gaseous medium of the chamber without stopping and give a broad signal ΔE in the energy spectrum. A large amount of them contributes to the coincident energy spectrum $E_2 + E_3$.

3) the α-particles of the natural radioactivity originating in the construction material of the chamber. These enter the gaseous medium with energies up to

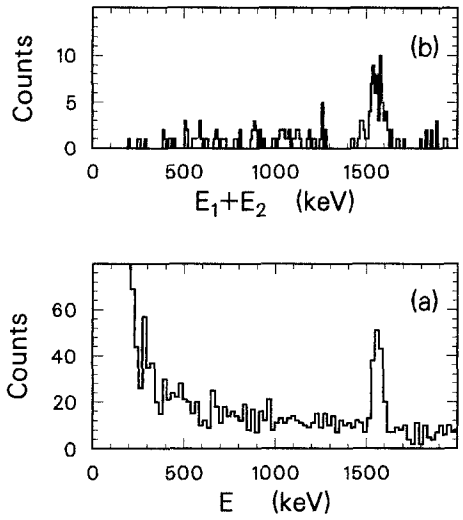

Fig. 2a and b. Energy spectrum of the 1.56 MeV protons from ^{53m}Co produced in $^{32}S+^{24}Mg$ reaction. In **a**: the anode is composed of one compartment; the low energy part of the spectrum is dominated by α-background. In **b**: the anode is composed of two concentric compartment; in this coincident spectrum between the two compartments, the α-background at low energy is strongly suppressed

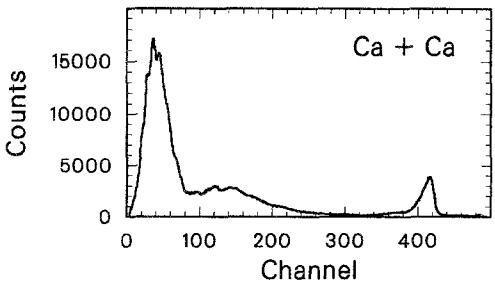

Fig. 3. Energy spectrum of the heavy ions given by the central compartment of the ionization chamber. These ions are focussed by Soleno and have lost a part of their energy in the crossing of the 2.1 μ havar window. The intense and wide peak at low energy corresponds to fusion evaporation residues, whereas the right hand side part corresponds to scattered beam

6 MeV, that they loose in the peripheral part of the chamber. Most of these particles are counted in the single spectrum E_3.

Before describing the experiment itself, let us outline the preliminary tests for the method of implantation and detection in a same gaseous medium controlled with a semirapid pulsation of the beam. The $^{24}Mg(^{32}S, p2n)$ reaction was used to produce ^{53}Co which is known to be emitter of 1.56 MeV protons from an isomeric state with a half-life of 250 ms. In a first test, the anode of the ionization chamber had only one compartment. The result of the measurement is given in Fig. 2a, where the peak of 1.56 MeV protons is clearly observed superimposed on α-background from natural radioactivity. In a second test, the anode was divided into two concentric compartments. The coincident spectrum between the two compartments is presented in Fig. 2b, where the peak of 1.56 MeV protons is seen on a almost suppressed background. The success of these two tests guided us to determine the conditions of the experiment itself which will be described hereafter.

Although the goal of the experiment was to explore the off-beam part of the time sequence, some care was taken in order to exploit in addition the on-beam part of the time. For this reason, CF_4 was chosen as gas of the ionization chamber and a havar foil of 2.1 μ was taken as an entrance window (both materials being free of hydrogen element), in order to avoid low-energy protons as recoil particles in scattering of ions focussed by the spectrometer.

Using a calcium target several runs were carried out with ^{32}S, ^{28}Si and ^{40}Ca beams taken at incident energies (deduced from calculations performed with Code ALICE [14]) which give the maximum production of ^{65}As, ^{69}Br and ^{77}Y respectively. For the ^{32}S and ^{40}Ca beams the gas pressure in the detector was set at 50 and 100 Torr successively and for ^{28}Si at only 100 Torr. In each measurement, the electric current of the spectrometer was set to focus the appropriate fusion residue. In fact, due to the broad charge and energy distributions, several charge states with different mean energies of this residue could be focussed at once. In Fig. 3, where is displayed an example of heavy ion energy spectrum, the focussed residues correspond to an intense broad peak at low energy. The control of the experiment was ensured by pulsers applied to the three anodes and in between runs the check of the ionization chamber was obtained by measuring the α spectrum from an ^{241}Am radioactive source. Two measurements of the background were made, one with the current of the spectrometer set on and the other without it. The main conditions of the experiment are given in Table 2 and commented below.

3. Experimental Results

The overall control of the experiment is illustrated in Fig. 4, where is plotted the off-beam $E_1+E_2+E_3$ spectrum from the $^{40}Ca(^{32}S, p2n)$ measurement performed at 100 Torr pressure of the detector. In this figure, histograms give the experimental results of $^{32}S+^{40}Ca$ reaction. The open circles display the results of the background measurement normalized to the same time duration. Solid circles represent the results of a calculation simulating the detection of delayed protons following the β decay of ^{69}Se, this

Table 2. Main characteristics and results of the performed measurements. The results into parentheses in the line of the $^{32}S+^{24}Mg$ reaction concern the 1.56 MeV protons emitted by the isomeric state of ^{53}Co. For other explanations, see the text

Fusion Evaporation Reactions						βp decay (p of ^{53m}Co)			p decay
Reaction	P(Torr)	E_i(MeV)	$n_i \times 10^{14}$	$n_{res} \times 10^6$	σ_f(mb)	$n_{\beta p}$	$\varepsilon_{\beta p}$	$\sigma_{\beta p}$(μb)	n_p for 1 μb
$^{32}S+^{24}Mg$	220 C_4H_{10}	92	4.4	58	580	(49)	(0.20)	(5.0)	
$^{28}Si+^{40}Ca$	100 CF_4	87	8.3	106	400	115	0.40	2.2	66
$^{32}S+^{40}Ca$	100 CF_4	99	4.2	61	300	384	0.36	10.6	50
	50 CF_4	99	2.7	51					42
$^{40}Ca+^{40}Ca$	100 CF_4	129	3.8	69	200	357	0.36	5.8	86
	50 CF_4	129	1.9	38					47

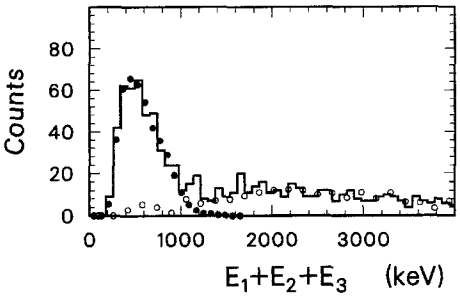

Fig. 4. Energy spectrum in $E_1+E_2+E_3$ for the $^{32}S+^{40}Ca$ reaction at 100 Torr, under a coincidence condition between anodes n° 2 and 3. The histogram is the result of the measurement. Open circles represent α-background normalized to the same time duration. Solid circles represent simulation calculation results for the β-delayed protons emitted by ^{69}Se

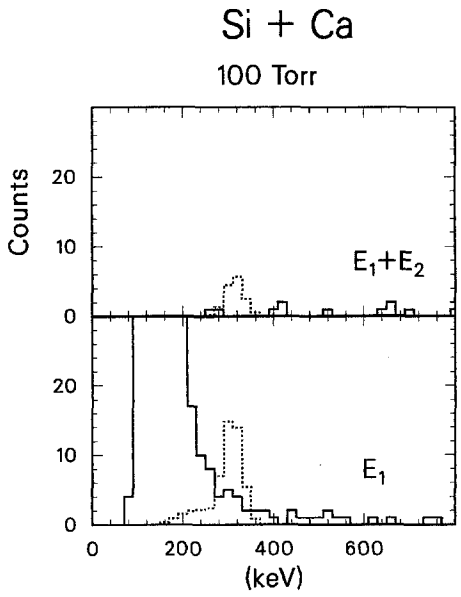

Fig. 5. Off-beam results for the search of a radioactivity proton ray from ^{65}As produced in $^{28}Si+^{40}Ca$ reaction, at 100 Torr pressure in the ionization chamber. Histograms are the experimental E_1 and E_1+E_2 spectra. Here, E_1 denotes the energy of a particle detected by anode n° 1 under an anticoincidence condition with respect to anodes n° 2 and 3, while E_1+E_2 denotes the sum of energies from anodes n° 1 and 2 under a coincidence condition between anodes n° 1 and 2 and an anticoincidence condition with respect to anode n° 3. The high number of events at $E \leqq 250$ keV in E_1 spectrum originates from β-radiation, whereas other events in E_1 and E_1+E_2 spectra are due to the general background, i.e., the β-delayed protons and α-natural radioactivity. Dotted lines are the results of a simulation calculation for a radioactivity proton ray at 300 keV from ^{65}As produced with a cross section of 1 μb (Table 2). No radioactivity proton-ray line is observed in the histogram

latter being supposed uniformely distributed inside the ionization chamber.

It is seen that the overall shape of the displayed spectrum is due to α-radiation from natural radioactivity and to β-delayed protons, both of them being mostly located in the E_2+E_3 spectrum. This shows that a double aim was achieved: *(i)* the possibility of removing these a priori unwanted events from the spectra of E_1 and E_1+E_2 where the radioactivity protons should be recorded, and *(ii)* the use of these events to monitor the experiment.

In fact, the radioactivity protons, which are searched for, should be equally located in the spectra of E_1 and E_1+E_2. The registered spectra are presented in Figs. 5–7 for the different reactions studied. On the left of these figures, are presented the spectra obtained at a pressure of 100 Torr in the detector, and on the right those obtained for 50 Torr. While histograms represent the measured events, dotted lines indicate the response (resulting from simulation) of the detection system to a proton ray of 300 keV originating from a proton radioactivity whose intensity corresponds to a production cross section of the emitting nucleus of 1 μb. One should notice that the existence of a proton radioactivity in a given reaction should yield a peak of about 80 keV FWHM at the same energy value in all of the four corresponding spectra, i.e., E_1 and E_1+E_2 for 100 and 50 Torr. None of the sets of spectra in Figs. 5–7 corresponding to

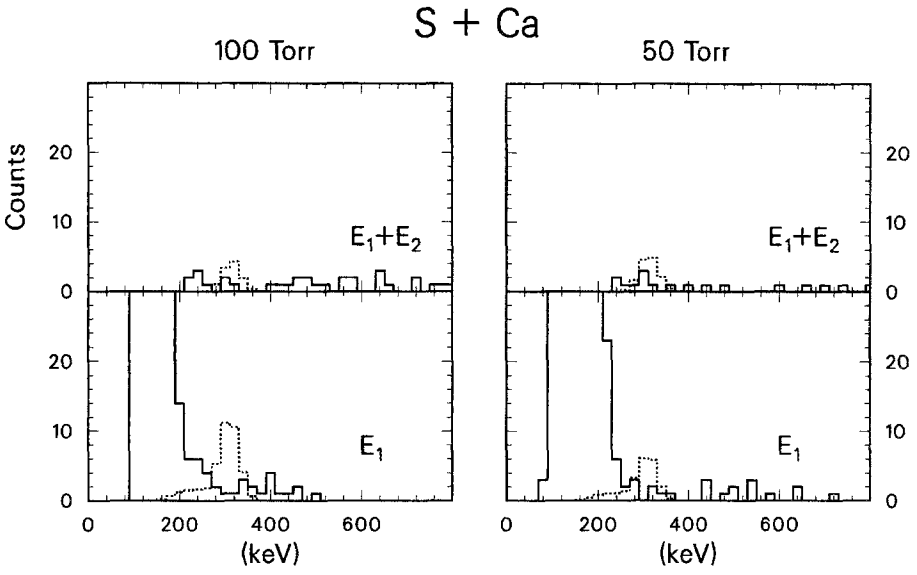

Fig. 6. Off-beam results for the search of a radioactivity proton ray from ^{69}Br produced in $^{32}S+^{40}Ca$ reaction, at 100 and 50 Torr pressure in the ionization chamber. Notations are similar to the ones of Fig. 5. No radioactivity protons are observed from ^{69}Br

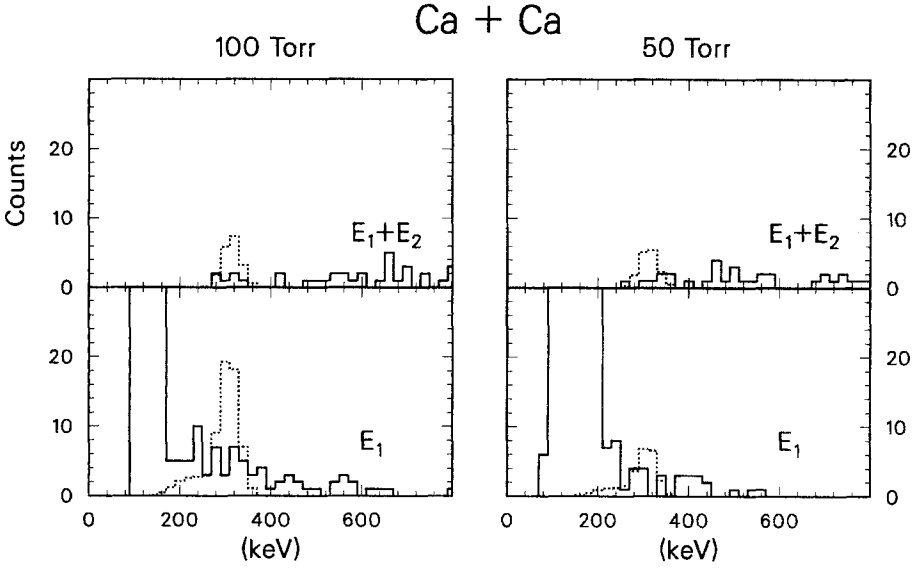

Fig. 7. Off-beam results for the search of a radioactivity proton ray from ^{77}Y produced in $^{40}Ca+^{40}Ca$ reaction, at 100 and 50 Torr pressure in the ionization chamber. Notations are similar to the ones of Fig. 5. No radioactivity protons are observed from ^{77}Y

the three reactions studied here shows a peak located between 250 and 600 keV. This experimental result excludes the existence of proton radioactivities from ^{65}As, ^{69}Br and ^{77}Y in the sensitivity range of our detection set up, in particular, a production cross section of 1 μb suggested by the simulation.

4. Discussion

The critical analysis and the sensitivity conditions of our study are based on the data summarized in Table 2. The six first columns of the table give for each measurement the general experimental conditions: *(a)* the pressure P used in the ionization chamber, *(b)* the incident energy E_i and the total number n_i of the projectiles, *(c)* the number n_{res} of residual nuclei implanted in the ionization chamber which is measured in the energy spectrum of heavy ions of anode n° 1 (Fig. 3) and *(d)* the fusion cross section σ_f taken from the tables of Wilcke et al. [15]. From these values together with the thickness of the target, one can deduce a value of ≈ 0.05 for the collection efficiency of Soleno, which is compatible with the result of other measurements [7].

Some data concerning the 1.56 MeV protons emitted by ^{53m}Co and the 1–3 MeV β-delayed protons emitted by ^{65}Ge, ^{69}Se and ^{77}Sr are presented in Table 2:

The numbers $n_{\beta p}$ of the β-delayed protons detected in each measurement is taken equal to the numbers of events in the bump at low energy in $E_1+E_2+E_3$ spectra similar to the one presented in Fig. 4.

The geometrical efficiency $\varepsilon_{\beta p}$ of the chamber for the detection of the β-delayed protons is calculated with the simulation program by assuming all of the residues as present in the gas and distributed uniformely. So calculated, the efficiency $\varepsilon_{\beta p}$ is slightly overestimated, because no account was taken for the residues evacuated in the continuous flow of the gaz or simply deposited behind the equipotential rings in the chamber.

The cross sections $\sigma_{\beta p}$ for the detection of the β-delayed protons were calculated using the expression

$$\sigma_{\beta p}=\frac{n_{\beta p}}{n_{\text{res}}}\cdot\sigma_f\cdot\frac{1}{\varepsilon_{\beta p}\cdot\varepsilon_t}$$

where the time efficiency ε_t is the fraction of time in which the β-delayed protons are detected; here, $\varepsilon_t=\frac{1}{2}$. Since there is no experimental value previously measured for $\sigma_{\beta p}$ to compare with, only comparison was made with expected values deduced from the production cross sections given by code ALICE and the measured βp branching ratios [9–13]. A satisfactory agreement in order of magnitude was obtained. For the 1.56 MeV protons emitted by ^{53}Co, σ_p is found to be 5 μb, a value that one could compare to the cross section of 8 μb previously reported from ^{16}O $+^{40}$Ca reaction [16].

In the last column of Table 2, are listed the values of the number n_p of expected radioactivity protons for a production cross section σ_p of 1 μb. The quantity n_p is calculated with the expression

$$\sigma_p=\frac{n_p}{n_{\text{res}}}\cdot\sigma_f\cdot\frac{1}{\varepsilon_p\cdot\varepsilon_{t'}}$$

where the geometrical efficiency ε_p is nearly equal to one, corresponding to a solid angle of about 4π, and the time efficiency $\varepsilon_{t'}$ varies with the half-life of the proton radioactivity, taking for instance the values, 0.27, 0.40, and $\approx$0.50 for $T_{\frac{1}{2}}=10$, 20 and $\geqq 50$ μs respectively. For the calculation of n_p, listed in Table 2, the product $\varepsilon_p\cdot\varepsilon_{t'}$ was taken equal to $\frac{1}{4}$. It is these values of n_p which are plotted with dotted lines in Figs. 5–7 to illustrate that a production cross section σ_p of 1 μb would give recognizable peaks in E_1 and E_1+E_2 spectra. As a consequence the sensitivity conditions defined for our measurements are: *(1)* an energy range of 250–600 keV, *(2)* a half-life range of 10 μs up to 100 ms and *(3)* a production cross section of 1 μb.

The energy range obtained here conveniently covers the expected one especially at low energy where a limit of 250 keV was reached for the three nuclei. This threshold is substentially lower than the value of 450 keV reported by Faestermann et al. [3] in their search for proton radioactivity in ^{77}Y.

The on-beam events recorded in our experiment allowed to extend the explored half-life range to a few μs but with a lower production cross section sensitivity due to a higher background originating from the beam. No evident proton rays have been seen.

Finally, the value of 1 μb for the production cross section sensitivity obtained here was one of the main goals of the experiment, based on the fact that the cross section values predicted by fusion evaporation codes [17] for ^{65}As, ^{69}Br and ^{77}Y production are higher by more than one order of magnitude.

5. Conclusion

The search for a proton radioactivity from ^{65}As, ^{69}Br and ^{77}Y nuclei in their ground states has been carried out, using fusion evaporation reactions to produce these proton rich nuclei and the spectrometer Soleno to collect them at zero degree. After various problems concerning the implantation into a gaseous detector and the selection of rare events have been solved, the investigation of proton radioactivity covered the ranges of 250–600 keV in energy and of 10 μs–100 ms in half-life. No such proton radioactivity has been observed within a cross section lower limit of 1 μb in the production of the emitter. Obviously, further investigation would require improvements to reach smaller fusion evaporation cross sections and shorter radioactivity half-lives. A different method which could be tried is to use fragmentation reactions as a production process, these reactions allowing in addition to study the nuclei of higher A ($80\leqq A\leqq 100$) non-attainable by fusion evaporation reactions with $Z=N$ projectiles and targets.

The good running of various systems was necessary in order to complete this work. We are indebted to several people for their close assistance: Mr J.C. Artiges, in the electronic system; Mr G. Renou, in the ionization chamber; Messrs A. Le Goff and G. Iltis, in the operation of the spectrometer Soleno. We also thank the crew of the target department for having provided us with high quality ^{24}Mg and Ca targets and the crew of the Tandem for the good running of the accelerator.

References

1. Hofman, S.: Particle emission from nuclei. Poenaru, D.N., Ivascu, M.S. (eds.), Vol. II, p. 25. Boca Raton, Florida, CRC Press 1989

2. Jackson, K.P., Clifford, E.T.H., Azuma, R.E., Faestermann, T., Schmeing, H.: Report AECL-5696, Atomic Energy of Canada, p. 24 (1976)
3. Faestermann, F., Gillitzer, A., Hartel, K., Kienle, P., Nolte, E.: Nuclei Far From Stability, Rosseau Lake, Ontario, AIP Conference Proceedings, **164**, 739 (1987)
4. Reiff, J.E., Hotchkis, M.A.C., Moltz, D.M., Lang, T.F., Robertson, J.D., Cerny, J.: Nucl. Instrum. Methods A **276**, 228 (1989)
5. Wapstra, A.H., Audi, G., Hoekstra, R.: At. Dat. Nucl. Data Tables **39**, 281 (1988)
6. Schapira, J.P., Azaiez, F., Fortier, S., Gales, S., Hourani, E., Kumpulainen, J., Maison, J.M.: Nucl. Instrum. Methods **224**, 337 (1984)
7. Hourani, E., Kumpulainen, J., Azaiez, F., Fortier, S., Gales, S., Maison, J.M., Massolo, P., Ramstein, B., Schapira, J.P.: Nucl. Instrum. Methods A **264**, 357 (1988)
8. Artiges, J.C., Richard, A.: SEP n° 221, Institut de Physique Nucléaire, B.P. n° 1, 91406 Orsay
9. Hardy, J.C., Macdonald, J.A., Schmeing, H., Faestermann, T., Andrews, H.R., Geiger, J.S., Graham, R.L.: Phys. Lett. **63** B, 27 (1976)
10. Macdonald, J.A., Hardy, J.C., Schmeing, H., Faestermann, T., Andrews, H.R., Geiger, J.S., Graham, R.L., Jackson, K.P.: Nucl. Phys. A **288**, 1 (1977)
11. Hardy, J.C., Faestermann, T., Schmeing, H., Macdonald, J.A., Andrews, H.R., Geiger, J.S., Graham, R.L., Jackson, K.P.: Nucl. Phys. A **371**, 349 (1981)
12. Vierinen, K.: Nucl. Phys. A **463**, 605 (1987)
13. Dessagne, Ph., Miehé, Ch., Baumann, P., Huck, A., Klotz, G., Ramdane, M., Walter, G., Maison, J.M.: Phys. Rev. C **37**, 2687 (1988)
14. Blann, M.: Overlaid ALICE, University of Rochester, Report n^0 C00-3493-29 (1976)
15. Wilcke, W.W., Birkelund, J.R., Wollersheim, H.J., Hoover, A.D., Huizenga, J.R., Schroder, W.U., Tubbs, L.E.: At. Data Nucl. Data Tables **25**, 389 (1980)
16. Jackson, K.P., Cardinal, C.U., Evans, H.C., Jelley, N.A., Cerny, J.: Phys. Lett. B **33**, 281 (1970)
17. Hofman, S.: Darmstadt, Calculation with Code HIVAP (Private communication)

E. Hourani, A. Elayi, S. Fortier,
S. Gales, J.M. Maison, A. Richard
Institut de Physique Nucléaire
B.P. No 1
F-91406 Orsay Cedex
France

Ph. Dessagne, Ch. Miehe
CRN
F-67037 Strasbourg Cedex
France

F. Asaiez
CENBG
Le Haut Vigneau
F-33170 Gradignan Cedex
France

P. Massolo
UNLP
RA-1900 La Plata
Argentina